Electronic Supplementary Material (ESI) for Materials Advances.
This journal is © The Royal Society of Chemistry 2023

Supporting Info

Impact of Thermal Gas Treatment on the Surface Modification of Li-Rich Mn-based Cathode Materials for Li-ion Batteries

Received 00th January 20xx,
Accepted 00th January 20xx

DOI: 10.1039/x0xx00000x

Maximilian Mellin,[a] Zhili Liang,[a] Hadar Sclar,[b] Sandipan Maiti,[b] Igor Píš,[c] Silvia Nappini,[c] Elena Magnano,[c,d] Federica Bondino,[c] Ilargi Napal,[c,e] Robert Winkler,[a] Réne Hausbrand,[a] Jan P. Hofmann,[a] Lambert Alff,[a] Boris Markovsky,[b] Doron Aurbach,[b] Wolfram Jaegermann,[a] and Gennady Cherkashinin.[a,*]

Table S1 Theoretical parameters used for the Mn $L_{3,2}$, Co $L_{3,2}$ and Ni $L_{3,2}$ edges simulations using CTM4XAS software.

	Symmetry	10Dq (eV)	$F_{d\text{-}d}$ (%)	$F_{p\text{-}d}$ (%)	$G_{p\text{-}d}$ (%)	Dt (eV)	Ds (eV)	Δ (eV)	$U_{d\text{-}d}$ (eV)	$U_{p\text{-}d}$ (eV)
Mn										
Mn^{2+} ref.75	O_h	1.2	80	80	80	-	-	7	0	0
Mn^{3+} ref.75	D_{4h}	1.54	65	75	75	0.02	0.06	4	0	0
Mn^{4+} ref.76	O_h	2.5	70	70	70	-	-	2.5	6.5	8.5
Co										
Co^{2+} ref.77	D_{4h}	-0.75	90	90	90	0	0.04	-	-	-
Co^{3+} ref.77	O_h	1.8	70	70	70	-	-	-	-	-
Ni										
Ni^{2+} ref.78	O_h	1.2	80	80	80	-	-	3	0	0

Here, $G_{p\text{-}d}$ is the reduction factor (%) of the exchange Coulomb, $F_{p\text{-}d}$ and $F_{d\text{-}d}$ are direct Coulomb Slater integrals. The Δ is the charge transfer parameter. The Dt, Ds and 10Dq are the crystal field parameters. $U_{d\text{-}d}$ and $U_{p\text{-}d}$ parameters correspond to 3d-3d and 2p-3d intra-atomic Coulomb interactions.

[a] Department of Materials and Earth Sciences, Technical University of Darmstadt, 64287 Darmstadt, Germany.
[b] Department of Chemistry, Bar-Ilan University, Ramat-Gan 5290002, Israel.
[c] IOM-CNRIstituto Officina dei Materiali, Strada Statale 14, km 163,5 in Area Science Park, 34149 Basovizza, Trieste, Italy.
[d] Department of Physics, University of Johannesburg, PO Box 524, Auckland Park, 2006, Johannesburg, South Africa.
[e] Università degli Studi di Trieste, Physics Department, P.le Europa 1, 34127 Trieste, Italy.
*Corresponding author: gennady.cherkashinin@tu-darmstadt.de
Electronic Supplementary Information (ESI) available: [details of any supplementary information available should be included here]. See DOI: 10.1039/x0xx00000x

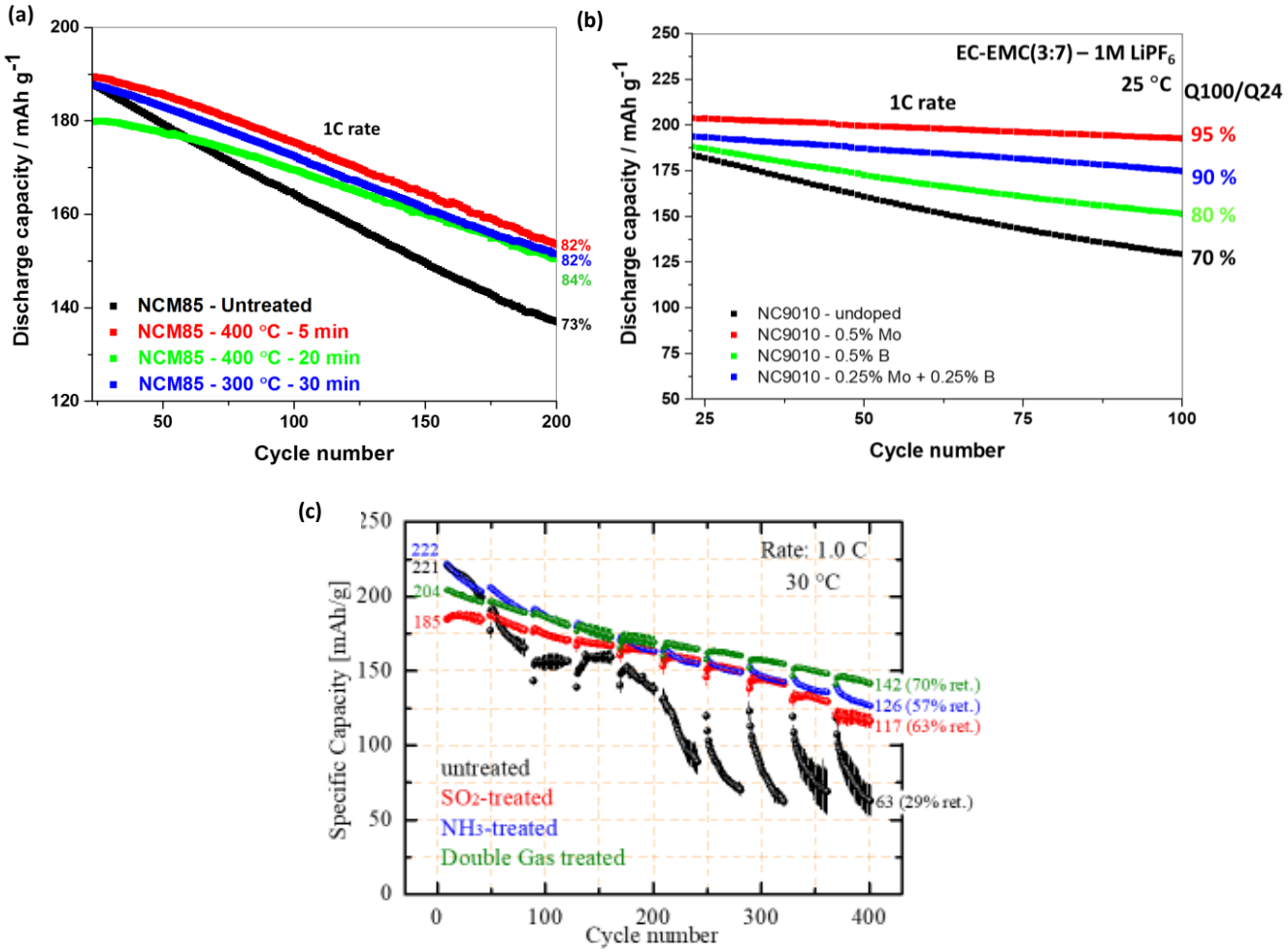

Figure S1. Cycling behaviour of electrodes comprising various materials: (a) $LiNi_{0.85}Co_{0.15}Mn_{0.05}O_2$ (NCM85) untreated and SO_2-gas treated for 5, 20 and 30 min, as indicated, ref. [S1], b) $LiNi_{0.9}Co_{0.1}O_2$ (NC9010) undoped, Mo-doped, B-doped and Mo-B-doped samples, ref. [S2], (c) HE-NCM untreated, SO_2-treated, NH_3-treated, and double-gas treated, ref. [S3].

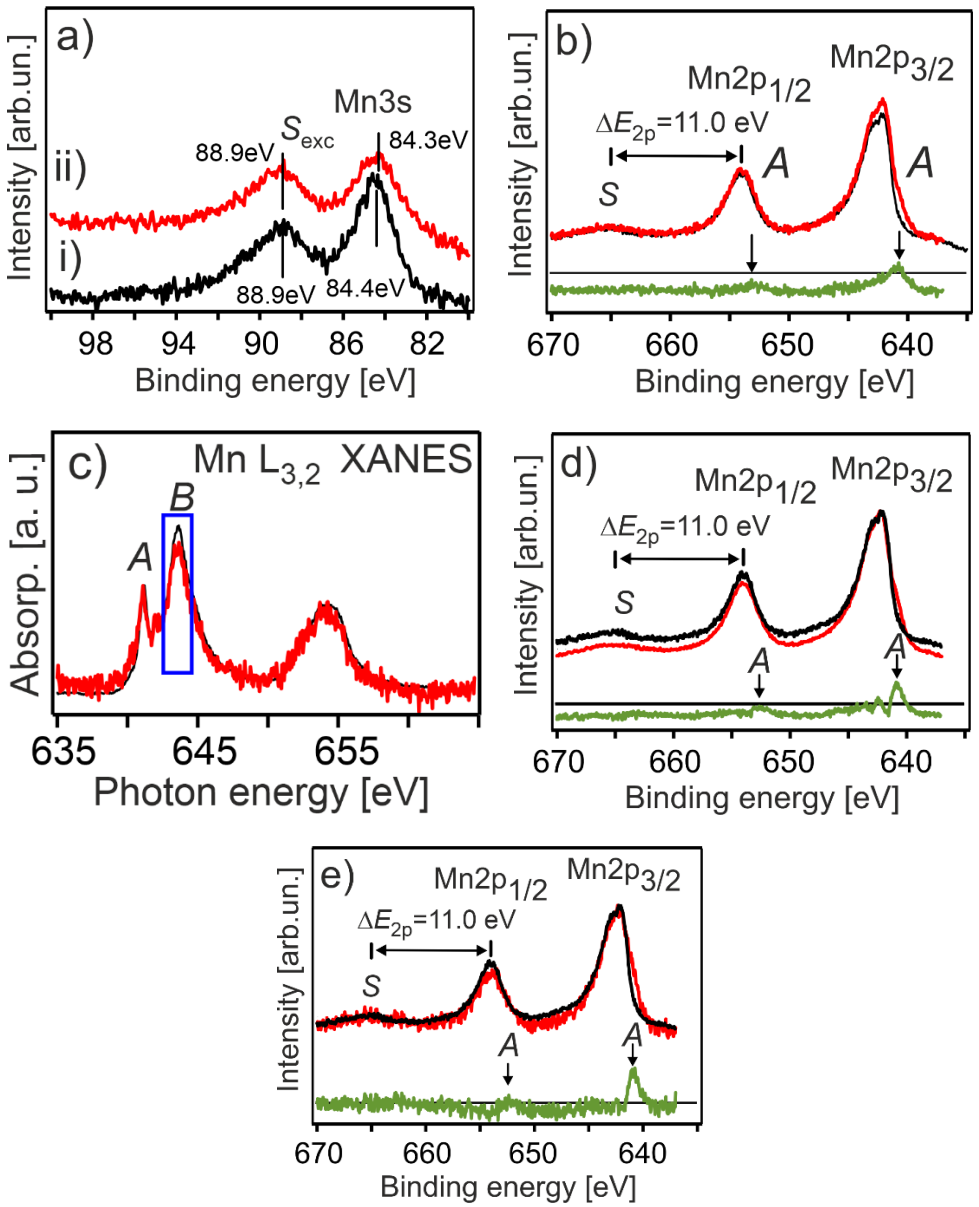

Figure S2. a) The Mn 3s photoelectron spectra of the *untreated HE-NCM*: *pristine* (without carbon and PVDF) (i) and *composite cathode* (with carbon and PVDF) (ii). The vertical lines show the binding energies of the main Mn 3s photoelectron peak and the exchange satellite, S_{exc}. The difference between Mn 3s and S_{exc} for the *pristine* and the *composite* cathode is ΔE_S ~ 4.5 eV and 4.6 eV, respectively. b) Mn 2p photoelectron spectra of the *untreated HE-NCM*: *pristine* (black line) and *composite cathode* (red line). c) Mn L edge of the *untreated HE-NCM*: *pristine* (black line) and *composite cathode* (red line) measured in the partial electron yield mode (PEY). The *B*/*A* ratio is lower for the *HE-NCM composite*, which is a sign of a partial reduction of Mn^{4+} ions. d) Mn 2p photoelectron spectra of the *untreated HE-NCM pristine* (black line) and *treated HE-NCM* without carbon and PVDF (red line). e) Mn 2p photoelectron spectra of the *untreated HE-NCM pristine* (black line) and the *treated HE-NCM composite cathode* (red line). The difference photoelectron spectra are shown in green with the vertical arrows pointing the spectral feature *A* different from Mn^{4+} state. All the spectra are normalized to their maximal intensity.

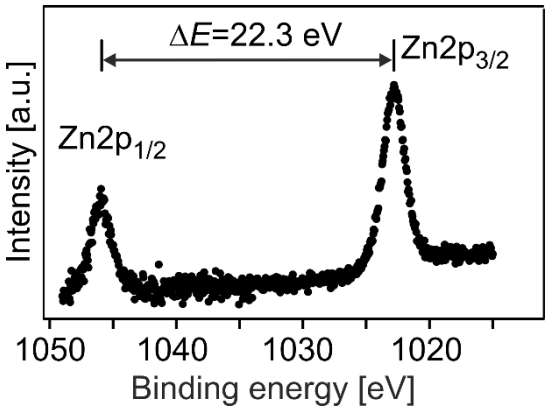

Figure S3. The Zn 2p photoemission of the HE-NCM double-gas (SO_2 and NH_3) treated composite cathode. The Zn $2p_{3/2}$ spectrum at E_{bin}~1022.8 eV evidences traces of $ZnSO_4$ (or $ZnCO_3$) at the surface of the HE-NCM.

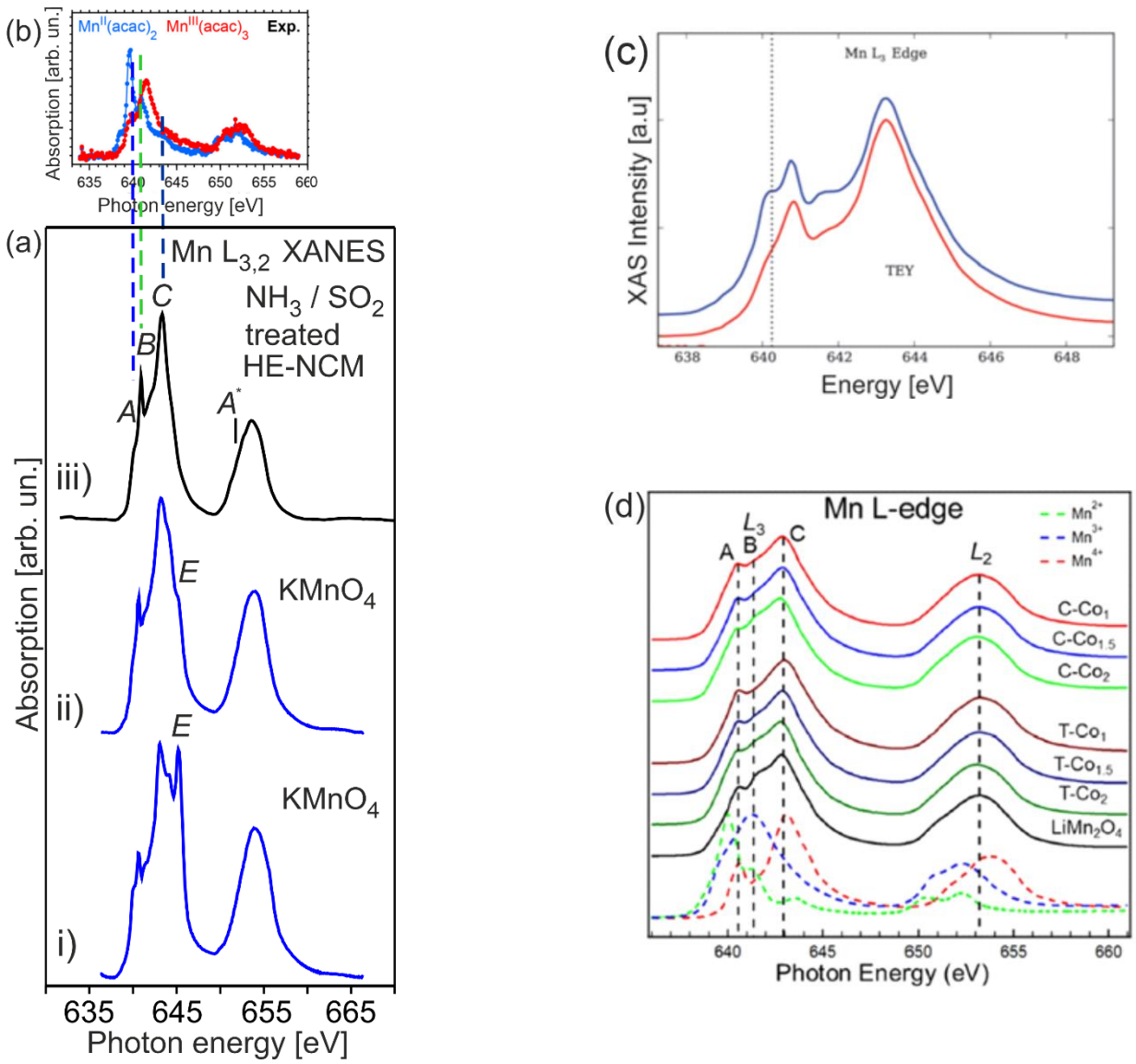

Figure S4. (a) Mn $L_{3,2}$ XANES of $KMnO_4$ (i, ii) and HE-NCM double-gas NH_3 and SO_2 treated composite cathode material (iii). The *E* spectral feature (i, ii) is characteristic for Mn^{7+} and it is strongly decreased in intensity as soon as Mn^{7+} state is photon reduced (ii). (b) $Mn^{II}(acac)_2$ and $Mn^{III}(acac)_3$ complexes in solution (Ref.[S4]). (c) Mn L_3 edge of NMC442 (blue) and NMC442-TiO_2 (red) after electrochemical cycling: dotted vertical line indicates the position of the +2 oxidation state (reproduced from Ref.[S5]). (d) Mn L edge of MnO (Mn^{2+}), Mn_2O_3 (Mn^{3+}) and Li_2MnO_3 (Mn^{4+}) shown by colour dashed lines, $LiMn_2O_4$ (black solid) and $Co_xMn_{3-x}O_4$ with x=1; 1.5; 2. C-Co_x and T-Co_x are cubic and tetragonal spinel, respectively (reproduced from Ref.[S6]).

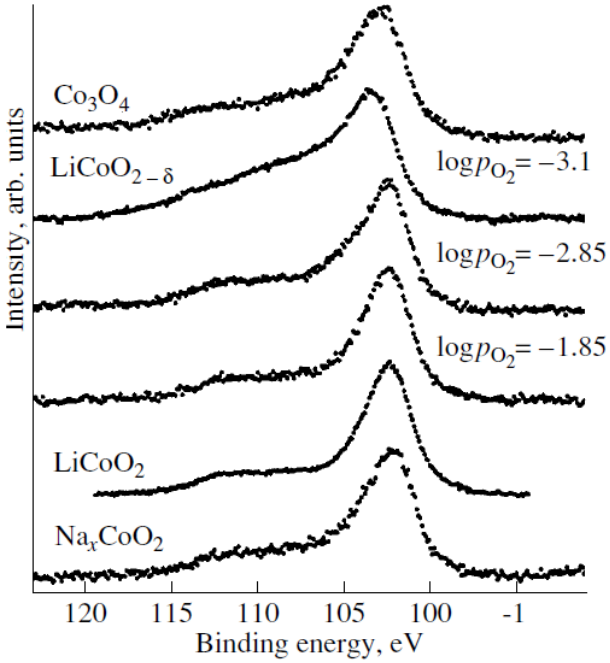

Figure S5. Co 3s photoemission and Co 2p X-ray emission spectrum (on the top) of various cobalt oxides adapted from Ref.[S7].

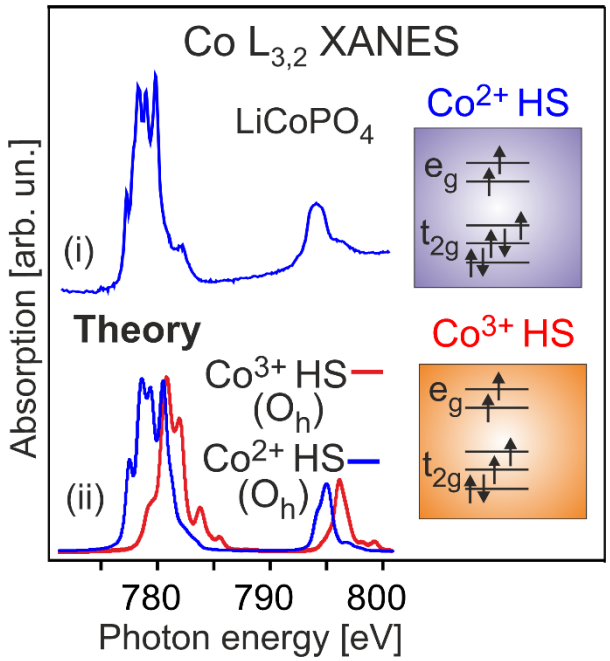

Figure S6. (a) Co $L_{3,2}$ XANES of a $LiCoPO_4$ thin-film cathode material (a, i). Theoretical calculations of the Co $L_{3,2}$ edges for the Co^{2+} with HS spin in O_h coordination geometry with np^6 $3d^6$ ground and np^5 $3d^7$ final states (a, ii) (see for details Ref.[S8]). The insert shows the electron configuration of Co^{2+} and Co^{3+} states in O_h symmetry.

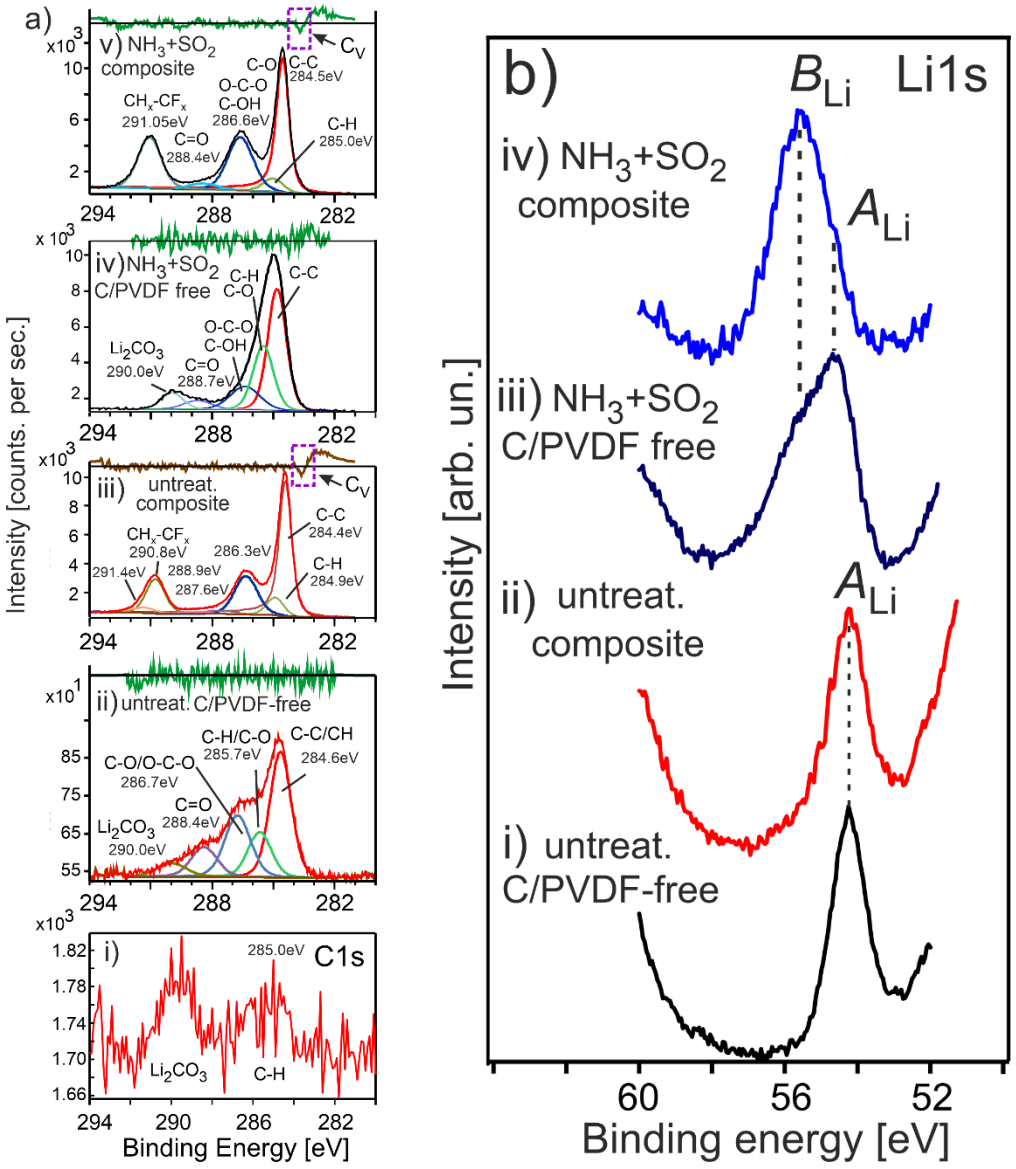

Figure S7. The C 1s (a) photoelectron spectra of (i) a $LiCoO^2$ thin film, (ii- v) HE-NCM vs. the treatment: (ii) *pristine*, (iii) *untreated composite*, (iv) *treated*, (v) *treated composite*. The green curve above the C 1s photoemission is the difference between the mathematical model and the result of the fitting procedure. A defect state C_V, highlighted with the frame, at E_{bin}~283.5 eV appears after mixing the HE-NCM active material with conductive carbon and PVDF (ii, iv). The procedure of fitting component peaks to reproduce experimental photoemission spectra utilizes mathematical algorithms to minimize a figure-of-merit as a measure of the closeness of the mathematic model to the experimental data [see description of a common fitting procedure in Ref.[S9]]. b) The normalized Li 1s photoelectron spectra of HE-NCM vs. the treatment: (i) *pristine*, (ii) *untreated composite*, (iii) *treated*, (iv) *treated composite*. The peak maxima and shoulder are labelled as A_{Li} (E_{bin}=54.2 eV (i, ii) and 54.7 eV (iii, iv)), and B_{Li} (E_{bin} =55.6 eV (iii, iv)).

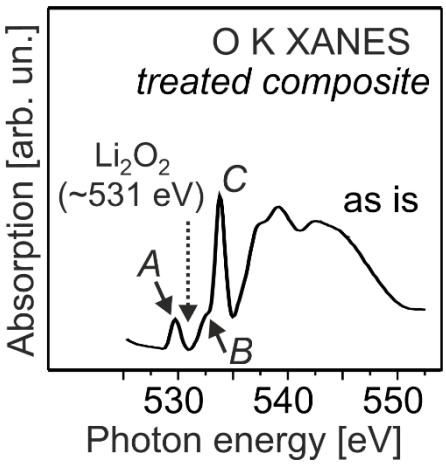

Figure S8. O K XANES of the as prepared *treated HE-NCM composite*. Li_2O_2, which is expected at ~531 eV [Ref. [S10]], is not detected.

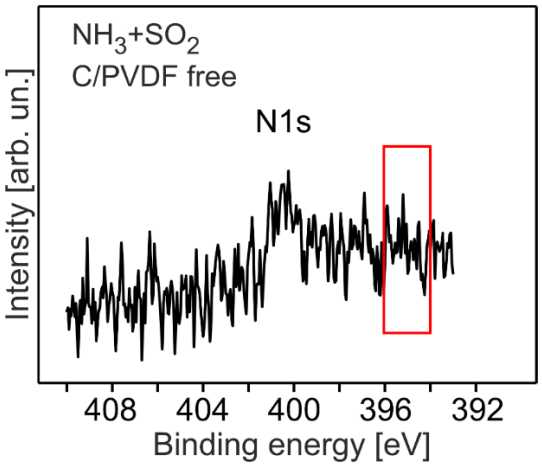

Figure S9. The N 1s photoelectron spectrum of the *treated HE-NCM*. The binding energy region of Li_3N is shown by the red rectangular.

References

S1 F. A. Susai, H. Sclar, S. Maiti, L. Burstein, O. Perkal, J. Grinblat, M. Talianker, S. Ruthstein, C. Erk, P. Hartmann, B. Markovsky and D. Aurbach, *ACS Appl. Energy Mater*., 2020, **3**, 3609.

S2 S. Maiti, H. Sclar, Rosy, J, Grinblat, M. Talianker, M. Tkachev, M. Tsubery, X. Wu, M. Noked, B. Markovsky and D. Aurbach, *Energy Storage Mater*., 2022, **45**, 74.

S3 F. A. Susai, A. Bano, S. Maiti, J. Grinblat, A. Chakraborty, H. Sclar, T. Kravchuk, A. Kondrakov, M. Tkachev, M. Talianker, D. T. Major, B. Markovsky and D. Aurbach, *J. Mater. Chem. A*, 2023, **11**, 12958.

S4 M. Kubin, M. Guo, M. Ekimova, M. L. Baker, T. Kroll, E. Källman, J. Kern, V. K. Yachandra, J. Yano, E. T. J. Nibbering, M. Lundberg and P. Wernet, *Inorg. Chem*., 2018, **57**, 5449.

S5 S. Wolff- Goodrich, F Lin, I. M. Markus, D. Nordlund, H. L. Xin, M. Asta and M. M. Doeff, *Phys. Chem. Chem. Phys*., 2015, **17**, 21778.

S6 X. Long, P. Yu, N. Zhang, C. Li, X. Feng, G. Ren, S. Zheng, J. Fu, F. Cheng and X. Liu, *Nanomater*. 2019, **9**, 577.

S7 V. R. Galakhov, V. V. Karelina, D. G. Kellerman, V. S. Gorshkov, N. A. Ovechkina and M. Neumann, *Phys. Solid State*, 2022, **44**(2), 266.

S8 G. Cherkashinin, R. Eilhardt, S. Nappini, M. Cococcioni, I. Pís, S. dal Zilio, F. Bondino, N. Marzari, E. Magnano and L. Alff, *ACS Appl. Mater. Interfaces*, 2022, **14**, 543.

S9 G. H. Major, N. Fairley, P. M. A. Sherwood, M. R. Linford, J. Terry, V. Fernandez and K. Artyushkova, *J. Vac. Sci. Technol. A*, 2020, **38**(6), 061203.

S10 R. Qiao, Yi.- D. Chuang, S. Yan and W. Yang, *PLOS ONE*, 2012, **7**(11), e49182.